

**A sparse discretisation for integral
equation formulations of high frequency
scattering problems**

Daan Huybrechs and Stefan Vandewalle

Report TW 447, January 2006



Katholieke Universiteit Leuven
Department of Computer Science
Celestijnenlaan 200A – B-3001 Heverlee (Belgium)

A sparse discretisation for integral equation formulations of high frequency scattering problems

Daan Huybrechs and Stefan Vandewalle

Report TW 447, January 2006

Department of Computer Science, K.U.Leuven

Abstract

We consider two-dimensional scattering problems, formulated as an integral equation defined on the boundary of the scattering obstacle. The oscillatory nature of high-frequency scattering problems necessitates a large number of unknowns in classical boundary element methods. In addition, the corresponding discretisation matrix of the integral equation is dense. We formulate a boundary element method with basis functions that incorporate the asymptotic behaviour of the solution at high frequencies. The method exhibits the effectiveness of asymptotic methods at high frequencies with only few unknowns, but retains the accurate convergence of the boundary element method for lower frequencies. New in our approach is that we combine this hybrid method with very effective quadrature rules for oscillatory integrals. As a result, we obtain a sparse discretisation matrix for the oscillatory problem. Moreover, the accuracy of a large part of the solution actually increases with increasing frequency. The sparse discretisation applies to problems where the phase of the solution can be predicted a priori, for example in the case of smooth and convex scatterers.

Keywords : oscillatory integral, steepest descent, numerical integration
AMS(MOS) Classification : Primary : 45B05, Secondary : 65D30, 41A60.

A sparse discretisation for integral equation formulations of high frequency scattering problems

Daan Huybrechs and Stefan Vandewalle

Katholieke Universiteit Leuven
Department of Computer Science
Celestijnenlaan 200A, B-3001 Leuven, Belgium.
{Daan.Huybrechs,Stefan.Vandewalle}@cs.kuleuven.be

Abstract

We consider two-dimensional scattering problems, formulated as an integral equation defined on the boundary of the scattering obstacle. The oscillatory nature of high-frequency scattering problems necessitates a large number of unknowns in classical boundary element methods. In addition, the corresponding discretisation matrix of the integral equation is dense. We formulate a boundary element method with basis functions that incorporate the asymptotic behaviour of the solution at high frequencies. The method exhibits the effectiveness of asymptotic methods at high frequencies with only few unknowns, but retains the accurate convergence of the boundary element method for lower frequencies. New in our approach is that we combine this hybrid method with very effective quadrature rules for oscillatory integrals. As a result, we obtain a sparse discretisation matrix for the oscillatory problem. Moreover, the accuracy of a large part of the solution actually increases with increasing frequency. The sparse discretisation applies to problems where the phase of the solution can be predicted a priori, for example in the case of smooth and convex scatterers.

1 Introduction

The accurate numerical modelling of physical problems involving strong oscillations is a challenging problem. Scattering problems in unbounded domains are often modelled by an integral equation defined on the boundary of the scattering obstacle. As such, the problem on an unbounded domain is reduced to a lower-dimensional problem on a bounded domain. Numerically, these are two important advantages. Still, the method has its drawbacks and difficulties arise as the frequency of the problem increases. Contrary to the case for partial differential equations, the discretisation matrix of an integral equation is dense. Furthermore, in order to represent an oscillatory solution, the number of unknowns in a boundary element approach has to be large. Typically, one chooses a fixed number of unknowns per wavelength per dimension. This results in a linear system with a very large and dense discretisation matrix. Hence, classical solution methods for scattering problems rapidly become prohibitively expensive [4].

Substantial efforts have been made over the last two decades to overcome these difficulties. One direction has been to improve on the solution time required to solve the dense linear

system. The Fast Multipole Method achieves a fast matrix-vector product in $O(N \log N)$ operations, when the number of unknowns N increases at least linearly with the wavenumber [15]. The fast matrix-vector product can be combined with a preconditioned iterative technique for an efficient overall solution algorithm [9]. Another direction is given by a number of asymptotic methods, such as geometrical optics, physical optics and the geometrical theory of diffraction [17, 23]. A common characteristic of asymptotic methods is that they have an error of the order $O(k^{-n})$, where k is the wavenumber and where the exponent n is typically equal to 1 or 2. This means that the accuracy of such methods improves with increasing frequencies. Asymptotic methods break down for low to moderate frequencies however.

A more recent trend is the combination of finite element methods with asymptotic methods. This is achieved by considering basis functions that are, e.g., piecewise polynomial, multiplied by the asymptotic form of the solution at large frequencies. The asymptotic behaviour of the solution to the problem of scattering by smooth convex obstacles was analysed in [27]. Motivated by these results, a hybrid scheme was considered in [1]. The authors report an overall solution method that requires $O(k^{1/3})$ operations as a function of the wavenumber, a huge improvement over the linear dependence on k . The basis functions are piecewise polynomials, multiplied by plane waves in a number of directions. Similar hybrid methods with even better results are proposed in [2, 7, 25, 24, 14, 11]. A number of operations that is independent of the wavenumber, for a fixed error, is achieved by Bruno, Geuzaine, Monro and Reitich in [7] for the scattering by smooth convex obstacles, and by Langdon and Chandler-Wilde in [25] for scattering on a half-plane. In the present paper, we combine a similar approach with recent insights in the behaviour of oscillatory integrals [21, 19]. As a result, we obtain a small, and highly sparse discretisation matrix. In addition, the accuracy of a large part of the solution actually *increases* with increasing frequency.

We start the paper in §2 with a review of quadrature rules for the evaluation of oscillatory integrals that have the general form

$$I[f] := \int_a^b f(x) e^{ikg(x)} dx, \quad (1)$$

where both f and g are smooth functions, and the wavenumber k determines the frequency of the oscillations. The review is based on results by Iserles and Nørsett in [20, 21] and by the authors in [19]. We show how Filon-type quadrature rules using derivatives can be constructed that have the form

$$I[f] \approx Q[f] := \sum_{i=0}^n \sum_{j=1}^{d_i} w_{i,j} f^{(j)}(x_i), \quad (2)$$

such that the accuracy of the rule improves with increasing frequency. This is quite contrary to the rapid deterioration of classical quadrature rules, based on polynomial interpolation, for increasingly oscillatory integrals. The asymptotic order of accuracy as a function of the frequency is $O(k^{-s-1})$, where the value of s depends on the number of derivatives used. This is much like the behaviour of truncated asymptotic expansions. However, due to the nature of the constructed rules, the result is exact for an arbitrarily large family of functions regardless of the frequency. The main difference with asymptotic expansions therefore is that there is no breakdown at low frequencies. In general, one can also expect a smaller error for moderate frequencies.

The results of [19] are generalised in §3 to an appropriately chosen model form

$$I_H[f] := \int_a^b f(x) H_\nu^{(1)}(kg_1(x)) e^{ikg_2(x)} dx,$$

where f , g_1 and g_2 are assumed to be smooth functions. The function $H_\nu^{(1)}(z)$ is the Hankel function of the first kind and order ν ; it is an oscillatory function for large arguments. The model form is chosen to represent the integrals that will appear later in the solution of scattering problems. The resulting quadrature rule has the same form as (2). The scattering problem is introduced in §4. The quadrature rules are subsequently used in the discretisation of the oscillatory integral equation in §5. We identify a setting in which each row of the discretisation matrix corresponds to the discretisation of a specific one-dimensional oscillatory integral with a known phase. Owing to the small number of quadrature points required for the evaluation of such integrals, the discretisation matrix is sparse. The accuracy of the solution improves because the quadrature rules themselves improve for increasing frequencies.

We illustrate the method with numerical results in §6. We consider the scattering of a plane wave and of a circular wave, by a circle and by an ellipse respectively. We end the paper with some concluding remarks in §7.

2 The efficient evaluation of oscillatory integrals

Traditionally, the evaluation of an oscillatory integral is considered to be a hard problem. The classical approach is to use a fixed number of quadrature points per wavelength, leading to a number of operations that scales linearly with the frequency. However, the asymptotic expansion of an oscillatory integral for large frequencies reveals that the value of the integral is determined by the behaviour of the integrand near a small set of special points [30, 6]. These are the boundary points of the interval, and the so-called *stationary points*. Consider the oscillatory integral (1), where both f and g are smooth functions. We call f the *amplitude*, and g the *oscillator* of the integral. The oscillatory nature is determined by the frequency parameter k . The stationary points of (1) are all solutions ξ to the equation $g'(\xi) = 0$, $\xi \in [a, b]$. A stationary point is said to have *order* r if $g^{(j)}(\xi) = 0$, $j = 1, \dots, r$, but $g^{(r+1)}(\xi) \neq 0$. The importance of such points lies in the fact that, locally, the integrand does not oscillate near a stationary point. Away from all stationary points and the boundary points a and b , the oscillations increasingly cancel out. This is reflected in the asymptotic expansion of (1). It can be shown that integral (1) with one interior stationary point of order r has an asymptotic expansion of the form [30]

$$I[f] \sim \sum_{j=0}^{\infty} \frac{c_j[f]}{k^{(j+1)/(r+1)}}, \quad k \rightarrow \infty. \quad (3)$$

It is proved in [21] that the first few coefficients $c_j[f]$ of the asymptotic expansion depend only on the first few derivatives of f and g , evaluated at the boundary points and at the stationary points. A number of recent methods exploit this behaviour, in order to obtain an approximation of $I[f]$ that improves with increasing k [21, 19, 26, 29]. We will recall two particularly useful approaches, that lead to a quadrature rule with a classical form. We refer the reader to [22] for a more general overview.

2.1 A Filon-type method

A well known approach for the evaluation of (1) is a *Filon-type method*. Assume

$$f(x) \approx \sum_{i=0}^n a_i[f] \phi_i(x),$$

i.e., the amplitude function can be approximated by a linear combination of given basis functions ϕ_i with coefficients $a_i[f]$ that depend on f . Then we have

$$I[f] \approx \sum_{i=0}^n w_i a_i[f], \quad \text{with } w_i := I[\phi_i].$$

Iserles and Nørsett proposed the use of a Hermite interpolating polynomial to approximate f in [20, 21]. This polynomial interpolates f and a number of derivatives in the endpoints and the stationary points of the interval $[a, b]$. It can be written as a linear combination of the derivatives of f with polynomial basis functions $\psi_{i,j}(x)$,

$$\psi(x) = \sum_{i=0}^n \sum_{j=0}^{d_i} f^{(j)}(x_i) \psi_{i,j}(x), \quad \text{with } \psi_{i,j}^{(j)}(x_i) = 1, \text{ and } \psi_{i,j}^{(l)}(x_k) = 0, (k, l) \neq (i, j).$$

The resulting quadrature rule has the form

$$Q_F[f] := \sum_{i=0}^n \sum_{j=0}^{d_i} w_{i,j}^F f^{(j)}(x_i), \quad \text{with } w_{i,j}^F = I[\psi_{i,j}]. \quad (4)$$

Assume that a stationary point x_i has order r_i . Then we choose to interpolate

$$d_i = (s-1)(r_i+1) \quad (5)$$

derivatives of f at x_i , with an integer $s > 0$. We interpolate $s-1$ derivatives in the endpoints, if they are not also stationary points. For this choice, one can show that

$$|I[f] - Q_F[f]| = O(k^{-s-1}), \quad k \rightarrow \infty. \quad (6)$$

It is said that the method has *asymptotic order* s . The proof is based on the fact that the first few coefficients of the asymptotic expansion of $I[f - \psi]$ vanish, because the first few derivatives of the interpolation error $e(x) = \psi(x) - f(x)$ are exactly zero in the interpolation points. A disadvantage of this method is that the weights need to be known analytically, or be computable by other means. Indeed, the integrals $w_{i,j}^F = I[\psi_{i,j}]$ are equally oscillatory as the original integral! This requirement is avoided in the so-called *Levin-type* methods [26, 29]. There, the integral is evaluated by solving a related non-oscillatory ordinary differential equation. Levin-type methods also exhibit high order accuracy for increasing frequencies [29]. However, these methods only give good results in the absence of stationary points; we will not consider them in detail.

2.2 A numerical steepest descent method

A different approach was introduced by the authors in [19], based on a numerical implementation of the method of steepest descent [6]. Justified by Cauchy's integral theorem for analytic functions, the integration path is deformed into a complex integration path that has better numerical properties. Specifically, the new path is chosen such that the integrand is not oscillatory along the path, and has exponential decay. The approach can be used to compute the weights of the Filon-type method. Alternatively, one can construct a different quadrature rule that has the same order of accuracy as (6).

Assume that both f and g are analytic functions. Subdivide the integration interval $[a, b]$ into subintervals $[a_i, b_i]$, $i = 1, \dots, l$, such that $g'(x) \neq 0$, $x \in (a_i, b_i)$, i.e., the oscillator g is a monotonic function on $[a_i, b_i]$. Then the inverse of g exists uniquely on $[a_i, b_i]$, and it is also analytic. We denote it by g_i^{-1} . The integral over $[a_i, b_i]$ is evaluated by deforming the integration path into the complex plane. Define the path $h_{x,i}(p)$ as

$$h_{x,i}(p) = g_i^{-1}(g(x) + ip), \quad x \in [a_i, b_i]. \quad (7)$$

This path is called the *path of steepest descent*. It follows immediately from the definition that $e^{ikg(h_{x,i}(p))} = e^{-kp}e^{ikg(x)}$. The line integral along the new integration path, originating in the point x and terminating in the point $h_{x,i}(P)$, can be written as

$$S_i[f; x] = e^{ikg(x)} \int_0^P f(h_{x,i}(p)) h'_{x,i}(p) e^{-kp} dp, \quad P > 0. \quad (8)$$

The integrand of (8) is not oscillatory, and decays exponentially fast. If f and g are analytic in a complex neighbourhood of $[a, b]$, then it is shown in [19] that the value of $I[f]$ can be approximated by

$$I[f] = \sum_{i=1}^l (S_i[f; a_i] - S_i[f; b_i]) + O(e^{-kd_0}), \quad (9)$$

with $P > 0$ and a real constant $d_0 > 0$. In many cases of practical interest, the limit case $P \rightarrow \infty$ is possible, and the error $O(e^{-kd_0})$ actually vanishes. In that case, decomposition (9) is exact.

The line integrals (8) can be evaluated efficiently using Gauss-Laguerre quadrature [10]. If x is not a stationary point, then

$$S_i[f; x] \approx Q_S[f; x, i] := \frac{e^{ikg(x)}}{k} \sum_{j=1}^n w_j f(h_{x,i}(p_j/k)) h'_{x,i}(p_j/k), \quad (10)$$

where w_j and p_j are the weights and quadrature points of a Gauss-Laguerre quadrature rule with n points. Approximation (10) has asymptotic order $2n$; it converges extremely fast. If a_i or b_i is a stationary point of order r , then the integrand has a singularity of the form $p^{1/(r+1)-1}$ as $p \rightarrow 0$. This singularity can be resolved using classical quadrature techniques [19]. The values $h_{x,i}(p_j/k)$ of the parameterisation of the path can be found by a small number of Newton-Raphson iterations to find the roots of

$$g(h_{x,i}(p)) - g(x) - ip = 0. \quad (11)$$

The derivatives of the parameterisation at the points p_j/k are found by taking the derivative of (11) with respect to p .

2.3 A localised Filon-type method

The approach of (9)-(10) can be used to compute the required moments of the form $I[\psi_{i,j}]$ of the Filon-type method. Owing to the decomposition as a *sum of contributions* of all the special points however, we can go one step further, and approximate the amplitude f *locally* near each special point a_i or b_i . Approximating f by its truncated Taylor series at each point x_i , we find a quadrature rule of the form

$$Q_L[f] := \sum_{i=0}^l \sum_{j=0}^{d_i} w_{i,j}^L f^{(j)}(x_i), \quad (12)$$

with $x_0 = a$, $x_i = b_i$, $i = 1, \dots, l$, and with the weights given by

$$\begin{aligned} w_{0,j}^L &= S_1 \left[\frac{(x-a)^j}{j!}; a \right], \\ w_{i,j}^L &= -S_i \left[\frac{(x-x_i)^j}{j!}; x_i \right] + S_{i+1} \left[\frac{(x-x_i)^j}{j!}; x_i \right], \quad i = 1, \dots, l-1, \\ w_{l,j}^L &= -S_l \left[\frac{(x-b)^j}{j!}; b \right]. \end{aligned}$$

The number of quadrature points and weights in (4) and (12) can be exactly the same: the quadrature points are the endpoints of the integration interval and the stationary points. The asymptotic order is the same too, under condition (5). The difference is that (12) does not require a global approximation of f , and that the weights are more easily computed. In a similar spirit, if the oscillator g is not analytic, it can be locally approximated near the special points by its truncated Taylor series. Convergence estimates for this approach are proved in [19]. Quadrature rule (12) hence applies to non-analytic functions f and g , provided they have a certain smoothness.

An important characteristic of the Filon-type quadrature rules (4) and (12) is that, by construction, they are exact for a number of polynomials up to a certain degree. Quadrature rule $Q_F[f]$ is exact for polynomials of degree

$$p = \left(\sum_{i=0}^n d_i + 1 \right) - 1. \quad (13)$$

Quadrature rule $Q_L[f]$ uses only local information, and is exact for polynomials of degree

$$p = \min_i d_i. \quad (14)$$

This means that, contrary to asymptotic expansions, both rules will converge for a large class of functions even at low frequencies. The quadrature rules combine the desirable numerical properties of classical quadrature rules and asymptotic expansions.

3 Specialised quadrature rules

The quadrature rules of the previous section apply only to the model integral (1). Intuitively however, one sees that the ideas can be readily generalised to any oscillatory integral. The

value of an oscillatory integral is determined by the behaviour of the integrand near the endpoints of the integration interval, and near the points where the integrand locally does not oscillate. In order to construct similar quadrature rules, one requires knowledge of the phase of the integral. In this section, we will construct such rules for a family of integrals that will arise in the scattering problem discussed later. In particular, the integrand involves an oscillatory Hankel function.

3.1 A generalised model form

Consider the oscillatory integral

$$I_H[f] = \int_a^b f(x) H_\nu^{(1)}(kg_1(x)) e^{ikg_2(x)} dx, \quad (15)$$

where f , g_1 and g_2 are smooth functions, and $H_\nu^{(1)}(z)$ is the Hankel function of the first kind of order ν . The Hankel function of order zero $H_0^{(1)}(z)$ has a logarithmic singularity at $z = 0$. Hankel functions of higher order have algebraic singularities of the form $1/z^\nu$, $z \rightarrow 0$ [3].

For large arguments, the Hankel functions behave like an oscillatory complex exponential with a decaying amplitude,

$$H_\nu^{(1)}(z) \sim \sqrt{\frac{2}{\pi z}} e^{i(z - \frac{1}{2}\nu\pi - 1/4\pi)}, \quad -\pi < \arg z < 2\pi, \quad |z| \rightarrow \infty. \quad (16)$$

Hence, the oscillator of the integrand of (15) is approximately given by

$$g(x) = g_1(x) + g_2(x), \quad (17)$$

up to the addition of a constant. The Hankel function decays exponentially fast for complex arguments with a positive imaginary part, as can be seen from the asymptotic behaviour (16). This means that the approach of §2.3 using the path of steepest descent is applicable. Hence, we may conjecture that a quadrature rule exists of the form

$$I_H[f] \approx Q_H[f] := \sum_{i=0}^l \sum_{j=0}^{d_i} w_{i,j}^H f^{(j)}(x_i). \quad (18)$$

In the remainder of the section, we will prove this conjecture, determine the quadrature abscissae x_i and show how the weights can be computed efficiently.

3.2 Construction of the quadrature rule

We start by stating some assumptions on the functions f and g . These assumptions are a.o. needed to guarantee the integrability and analyticity of the integrand in (15). First, we assume that f is analytic in an open complex neighbourhood D of $[a, b]$, so that $[a, b] \subset \text{int } D$. Likewise, we assume that g_1 and g_2 are non-singular and analytic in D , except possibly along a branch cut that extends from a or b to the boundary of the region D , i.e., a and b may be branch points but not singular points. We assume furthermore that $g(x)$, defined by (17), is strictly monotonic on the open interval (a, b) and hence invertible, but possibly $g'(a) = 0$ or

$g'(b) = 0$. Also, we assume that $g_1(x) \neq 0$, $x \in (a, b)$. Finally, if $\nu > 0$ and $g_1(\xi) = 0$ we assume that f behaves like

$$f(x) \sim (x - \xi)^{\nu-1+\epsilon}, \quad x \rightarrow 0, \quad \text{with } \epsilon > 0. \quad (19)$$

Condition (19) guarantees that the integrand of $I_H[f]$ is integrable. Subject only to condition (19) and the analyticity requirements, the integration interval of (15) can always be split into a number of subintervals that satisfy the conditions. The assumptions guarantee that the integrand of $I_H[f]$ is analytic on $[a, b]$ except possibly in the points a and b . In particular, this will allow us to apply Cauchy's integral theorem to select the integration path of (15).

Theorem 3.1. *Under the assumptions stated above, the integral $I_H[f]$ can be approximated by a sum of contributions*

$$I_H[f] = S^H[f; a] - S^H[f; b] + O(e^{-kd_0}), \quad (20)$$

with $d_0 > 0$, and with the contributions given by the integrals

$$S^H[f; x] = \int_0^P f(h_x(p)) H_\nu^{(1)}(kg_1(h_x(p))) e^{ikg_2(h_x(p))} h'_x(p) dp, \quad (21)$$

where $h_x(p)$ satisfies

$$g(h_x(p)) = g(x) + ip. \quad (22)$$

The proof is almost identical to the proof of Lemma 4.1 in [18] and is omitted; it differs mainly in the special treatment of the Hankel function based on the asymptotic expression (16).

We note from the asymptotic behaviour (16) that the integrand of the line integral $S^H[f; x]$ in (21) is non-oscillatory and exponentially decaying in the integration variable p ,

$$H_\nu^{(1)}(kg_1(h_x(p))) e^{ikg_2(h_x(p))} \sim \sqrt{\frac{2}{\pi kg_1(h_x(p))}} e^{ikg(x)} e^{i(-\frac{1}{2}\nu\pi-1/4\pi)} e^{-kp}, \quad k \rightarrow \infty.$$

The size of the constant d_0 is related to the size of the region of analyticity of f and g [18]. In the numerical examples of the scattering problem, given in §6, we will be able to choose the limit case $P = \infty$. The error of decomposition (20) then vanishes even at low frequencies.

We proceed in a similar way as in §2.3. Since f is analytic in D , it has an absolutely convergent Taylor series. By the linearity of S^H , we may write

$$S^H[f; x_0] = \sum_{j=0}^{\infty} f^{(j)}(x_0) S^H \left[\frac{(x - x_0)^j}{j!}; x_0 \right].$$

Now, consider a subdivision of $[a, b]$ into subintervals $[a_i, b_i]$, $i = 1, \dots, l$, such that on each subinterval the conditions of Theorem 3.1 are satisfied. Truncating the Taylor series of f at each special point a_i and b_i after a finite number of terms, we arrive at a quadrature rule $Q_H[f]$ of the form (18), with weights given by

$$w_{0,j}^H = S_1^H \left[\frac{(x - a)^j}{j!}; a \right], \quad (23)$$

$$w_{i,j}^H = -S_i^H \left[\frac{(x - x_i)^j}{j!}; x_i \right] + S_{i+1}^H \left[\frac{(x - x_i)^j}{j!}; x_i \right], \quad i = 1, \dots, l - 1, \quad (24)$$

$$w_{l,j}^H = -S_l^H \left[\frac{(x - b)^j}{j!}; b \right]. \quad (25)$$

The weights can be explicitly computed very efficiently, by using Gauss-Laguerre quadrature or similar techniques. The accuracy of these methods improves rapidly as a function of k , due to the faster decay of the integrands as k increases. For the purposes of our application, this advantageous characteristic is not even needed. It suffices already that the number of operations for a fixed accuracy is bounded with respect to k . We therefore choose to focus on the convergence properties of the quadrature rule itself, rather than on the convergence of methods to compute the weights.

3.3 Convergence properties of the quadrature rule

We discuss the properties of the specialised quadrature rule $Q_H[f]$ as a function of k . It is clear that the rule is exact by construction for polynomials of degree less than or equal to

$$p = \min_i d_i. \quad (26)$$

For more general functions, the accuracy as a function of k is determined by the asymptotic size of the weights. We will show that the size of the weights decreases both with increasing frequency and with increasing order of the corresponding derivative. The order of accuracy of the quadrature rule is therefore equal to the asymptotic size of the first weight that is discarded by truncation. In order to quantify this size, we require a few technical lemmas.

Lemma 3.2. *Assume x_0 is a stationary point that has order r . The parameterisation of the path (22) behaves as*

$$h_{x_0}(p) = x_0 + O(p^{1/(r+1)}), \quad p \rightarrow 0, \quad (27)$$

$$h'_{x_0}(p) = O(p^{1/(r+1)-1}), \quad p \rightarrow 0. \quad (28)$$

Proof. Since $g^{(j)}(x_0) = 0$, $j = 1, \dots, r$, we can write the Taylor series of g as

$$g(x) = g(x_0) + g^{(r+1)}(x_0) \frac{(x - x_0)^{r+1}}{(r+1)!} + O((x - x_0)^{r+2}).$$

The path $h_{x_0}(p) = g^{-1}(g(x) + ip)$ solves $g(h_{x_0}(p)) = g(x) + ip$, and hence

$$h_{x_0}(p) \sim x_0 + \sqrt[r+1]{\frac{ip(r+1)!}{g^{(r+1)}(x_0)}}, \quad p \rightarrow 0. \quad (29)$$

The second result follows by differentiation. Note that the complex root is multi-valued: the correct root is selected by using the analytic continuation of the inverse g_i^{-1} that satisfies $g_i^{-1}(g(x)) = x$ on $[a_i, b_i]$ in expression (22). \square

The size of the weights follows from the size of the line integrals $S^H \left[\frac{(x-x_0)^j}{j!}; x \right]$. Recall that the integral may be singular if $g_1(x) = 0$. We will assume for the sake of brevity that, in that case, $g'_1(x) \neq 0$. This condition is always satisfied by the applications in §6.

Lemma 3.3. *Let $S^H[f; x]$ be defined by (21) with $P = \infty$, and g defined by (17). Assume that $g'(x_0) \neq 0$, i.e., x_0 is not a stationary point. If $g_1(x_0) \neq 0$, we have*

$$|S^H[(x - x_0)^j; x_0]| = O(k^{-j-3/2}), \quad k \rightarrow \infty.$$

If $g_1(x_0) = 0$ and $g'_1(x_0) \neq 0$, the integral is singular and we have

$$|S^H[(x - x_0)^j; x_0]| = O(k^{-j-1}), \quad j \geq \nu, \quad k \rightarrow \infty.$$

Proof. We write the integral $S^H[(x - x_0)^j; x_0]$ as

$$S^H[(x - x_0)^j; x_0] = \int_0^\infty u(p)e^{-kp} dp = \frac{1}{k} \int_0^\infty u(q/k)e^{-q} dq, \quad (30)$$

with

$$u(p) = (h_{x_0}(p) - x_0)^j h'_{x_0}(p) H_\nu^{(1)}(kg_1(h_{x_0}(p))) e^{ikg_2(h_{x_0}(p))} e^{kp}. \quad (31)$$

It is a consequence of Watson's Lemma that the asymptotic expansion of the integral can be obtained by integrating the asymptotic expansion of $\frac{1}{k}u(q/k)$ as $k \rightarrow \infty$ term by term in (30) [6, 31]. Generalising Watson's Lemma, this remains true for integrals of the form $\int_0^\infty u(p)h(kp)dp$ where $h(z) \sim \log(z)^n z^s e^{-z}$, $n \geq 0$, $s \in \mathbb{Z}$, $z \rightarrow 0$, if the integrand is integrable [5]. This means that the singularity of the Hankel function has no influence on the asymptotic expansion.

First, consider the case $g_1(x_0) \neq 0$. Then, combining the asymptotic behaviour of the Hankel function for large arguments (16) with the results (27)-(28) of Lemma 3.2 for $r = 0$, we have $u(q/k) \sim k^{-j-1/2}$. From (30) we can conclude $|S^H[(x - x_0)^j; x_0]| = O(k^{-j-3/2})$.

Next, consider the case $g_1(x_0) = 0$. If $g'_1(x_0) \neq 0$, then we have $g_1(h_{x_0}(p)) \sim p^{1/(r+1)} = p$. It follows that $H_\nu^{(1)}(kg_1(h_{x_0}(q/k))) = O(1)$, $k \rightarrow \infty$. Hence, by the generalisation of Watson's Lemma, we may conclude $|S^H[(x - x_0)^j; x_0]| = O(k^{-j-1})$, $j \geq \nu$. \square

The corresponding lemma for stationary points is very similar. The difference is due to the different behaviour of the parameterisation as described by Lemma 3.2.

Lemma 3.4. *Let $S^H[f; x]$ be defined by (21) with $P = \infty$, and g defined by (17). Assume that x_0 is a stationary point of order r . If $g_1(x_0) \neq 0$, then we have*

$$|S^H[(x - x_0)^j; x_0]| = O(k^{-(j+1)/(r+1)-1/2}), \quad k \rightarrow \infty.$$

If $g_1(x_0) = 0$ and $g'_1(x_0) \neq 0$ then we have

$$|S^H[(x - x_0)^j; x_0]| = O(k^{-(j+1+r/2)/(r+1)}), \quad j \geq \nu, \quad k \rightarrow \infty.$$

Proof. Consider again the function $u(p)$, given by (31). Assume first that $g_1(x_0) \neq 0$. We have $(h_{x_0}(q/k) - x_0)^j \sim k^{-j/(r+1)}$ and $h'_{x_0}(q/k) \sim k^{r/(r+1)}$. Since $kg_1(h_{x_0}(q/k)) \sim kg_1(h_{x_0}(0)) = kg_1(x_0)$, we also have $H_\nu^{(1)}(kg_1(h_{x_0}(q/k))) \sim k^{-1/2}$. Combined in (30), and by applying Watson's Lemma, this yields the first result.

The case where $g_1(x_0) = 0$ is slightly different. Since $g'_1(x_0) \neq 0$, we have $g_1(h_{x_0}(q/k)) \sim k^{-1/(r+1)}$ and, hence, $kg_1(h_{x_0}(q/k)) \sim k^{r/(r+1)}$. The Hankel function therefore yields the factor $k^{-(r/2)/(r+1)}$ instead of $k^{-1/2}$ as in the first case. \square

The convergence of the quadrature rule (18) as a function of k can now be established. Note that the results of Lemma 3.3 agree with those of Lemma 3.4 if we take the order of a regular point to be $r = 0$. Hence, we need not distinguish between stationary points and regular (end)points.

Lemma 3.5. *The error of the approximation of $S_i^H[f; x_0]$, $x_0 \in [a_i, b_i]$, is*

$$|S_i^H[f; x_0] - Q_i^S[f; x_0]| = \left| S_i^H[f; x_0] - \sum_{j=0}^{d_i} w_{i,j}^H f^{(j)}(x_0) \right| = O(k^{-\alpha_i}), \quad k \rightarrow \infty. \quad (32)$$

If $g_1(x_0) \neq 0$ then $\alpha_i := (d_i + 2)/(r + 1) - 1/2$. If $g_1(x_0) = 0$ and $g_1'(x_0) \neq 0$, then $\alpha_i := (d_i + 2 + r/2)/(r + 1)$.

Proof. Since the weights decay as a function of k , and as a function of the order of derivative j , the error of the quadrature scheme is asymptotically determined by the size of the first discarded weight. The result follows from Lemma's 3.3 and 3.4 by setting $j = d_i + 1$. \square

The theorem that characterises the accuracy of the complete quadrature rule follows immediately.

Theorem 3.6. *Consider the approximation of $I_H[f]$ by $Q_H[f]$. The error has asymptotic order $\alpha - 1$ with $\alpha = \min_i \alpha_i$, and where α_i is specified in Lemma 3.5.*

As an example, we consider the integral $\int_0^1 \cos(x - 1) H_0^{(1)}(kx) e^{ik(x^2 + x^3 - x)} dx$. The total oscillator for this integral is $g(x) = x^2 + x^3$. There are two quadrature points: there is a singularity and a stationary point of order 1 at $x = 0$, and a regular endpoint at $x = 1$. The weights $w_{0,j}^H$ and $w_{1,j}^H$ are given by (23) and (25) respectively. From Lemma 3.4 we have $|w_{0,j}^H| = O(k^{-(j+1)/2-1/4})$ and from Lemma 3.3 we have $|w_{1,j}^H| = O(k^{-j-3/2})$. Using d_0 and d_1 derivatives, the error has order $\min\{O(k^{-(d_0+2)/2-1/4}), O(k^{-(d_1+1)-3/2})\}$ by Theorem 3.6. We choose $d_1 = \max\{0, \lceil (2d_0 - 5)/4 \rceil\}$ to match the errors. Table 1 shows the convergence of the quadrature rule $Q_H[f]$ as a function of k and d_0 .

Table 1: Absolute error of the approximation of $I_H[f]$ by $Q_H[f]$, with $f(x) = (x-1)$, $g_1(x) = x$ and $g_2(x) = x^2 + x^3 - x$. The last row shows the value of $\log_2(e_{400}/e_{800})$: this value should approximate $d_0/2 + 5/4$.

$k \setminus d_0$	0	1	2	3
100	$1.2E - 3$	$2.8E - 5$	$1.3E - 6$	$2.6E - 8$
200	$5.1E - 4$	$8.6E - 6$	$2.9E - 7$	$4.1E - 9$
400	$2.2E - 4$	$2.6E - 6$	$6.4E - 8$	$6.2E - 10$
800	$9.3E - 5$	$7.8.1E - 7$	$1.4E - 8$	$9.7E - 11$
rate	1.23	1.73	2.20	2.68

4 High frequency scattering problems

4.1 Problem statement

We are interested in the solution of the two-dimensional Helmholtz equation in the domain $\Omega^+ = \mathbb{R}^2 \setminus \overline{\Omega}$ that is exterior to the open domain Ω , subject to a Dirichlet boundary condition on the boundary $\Gamma = \partial\Omega$. The domain Ω represents an obstacle that scatters an incoming

acoustic or electromagnetic wave [8, 28]. The exterior Dirichlet problem has a unique solution and can formally be stated as follows.

Problem 4.1. *Find a function $u \in C^2(\Omega^+) \cap C(\overline{\Omega^+})$ such that*

$$\begin{aligned} \Delta u(x) + k^2 u(x) &= 0, & x \in \Omega^+, \\ u(x) &= 0, & x \in \Gamma = \partial\Omega^+. \end{aligned}$$

and the function u satisfies the Sommerfeld radiation condition at infinity given by

$$\left| \frac{\partial u}{\partial r} - iku \right| = o(1/\sqrt{r}), \quad \text{with } r := \|x\| \rightarrow \infty.$$

The Helmholtz equation models the scattering of time-harmonic waves of the form $u(x)e^{-i\omega t}$. In the absence of damping we have $k = \omega/c$, with c the speed of propagation. For the scattering of an incoming wave $u^i(x)$ by the obstacle Ω , the solution can be written as $u(x) = u^i(x) + u^s(x)$. The function $u^s(x)$ represents the scattered wave; it satisfies the Helmholtz equation with the Dirichlet boundary condition $u^s(x) = -u^i(x)$ on Γ .

The scattered wave can be represented in terms of the *single-layer potential*,

$$(Sq)(x) = \int_{\Gamma} K(x, y)q(y) \, ds_y, \quad \text{with } K(x, y) = \frac{i}{4}H_0^{(1)}(k|x - y|), \quad (33)$$

where q is the *density function* defined on the boundary Γ , and where $K(x, y)$ is the *fundamental solution* or *Green's function* of the two-dimensional Helmholtz equation. It can be shown that the single-layer potential satisfies the Sommerfeld radiation condition and the Helmholtz equation outside Ω . The scattered wave due to an incoming wave u^i is given by $u^s = -Sq$, if the density function q is found as the solution to the *Fredholm integral equation of the first kind*

$$(Sq)(x) = u^i(x), \quad x \in \Gamma. \quad (34)$$

Due to the existence of a countable number of resonant frequencies for the interior Dirichlet problem of the Laplacian Δ , integral equation (34) is not always solvable. In particular, equation (34) is not solvable for wavenumbers k such that $-k^2$ is an eigenvalue of Δ , i.e., $\Delta u = -k^2 u$ in Ω , with $u(x) = 0$ on Γ . In that case, the density function can be found as the solution to the *Fredholm integral equation of the second kind*

$$\frac{q(x)}{2} + \int_{\Gamma} \left(\frac{\partial K}{\partial n_x}(x, y) + i\eta K(x, y) \right) q(y) \, ds_y = \frac{\partial u^i}{\partial n}(x) + i\eta u^i(x), \quad x \in \Gamma. \quad (35)$$

The notation $\frac{\partial}{\partial n_x}$ is used to denote the normal derivative with respect to the variable x . Equation (35) is called the *combined field integral equation* [16]. The equation is uniquely solvable for all values of the wavenumber k if the *coupling parameter* η is real and non-zero.

An important observation is that $q = \frac{\partial u}{\partial n}$, i.e., the density function is exactly the (exterior) normal derivative of the solution to Problem 4.1. This means that the solution to equations (34) and (35) is directly related to a physical property of the problem. For example, in electromagnetics, the normal derivative of the electric field is proportional to the induced current on the surface of the conducting obstacle [28].

4.2 High frequency integral equation formulation

The density function q is highly oscillatory for large values of the wavenumber k . The solution of equations (34) or (35) therefore requires, generally, a large number of unknowns. In some cases however, one has a priori information about the phase of the solution. For example, if the obstacle is convex, and if the incoming wave is a plane wave, then the phase of the solution q is approximately the same as the phase of the incoming wave. Assume the incoming wave is $u^i(x) = u_s^i(x)e^{ikg^i(x)}$. Then we can write

$$q(x) = q_s(x)e^{ikg^i(x)}, \quad x \in \Gamma, \quad (36)$$

where $q_s(x)$ is a non-oscillatory function, at least approximately. In physical terms, the oscillations of the induced current on a perfectly conducting surface tend to follow the oscillations of the incoming electromagnetic wave. This is the reason why the problem should be formulated such that the solution q corresponds to a physical variable - only in that case is the phase known in the form of (36). This was noted in [7]; the integral equation formulation of this section follows the same pattern as [7].

Substituting (36) in (34) yields

$$\int_{\Gamma} \frac{i}{4} H_0^{(1)}(k|x-y|) q_s(y) e^{ikg^i(y)} ds_y = u^i(x) = u_s^i(x) e^{ikg^i(x)}.$$

Dividing by the oscillatory factor in the right hand side, and introducing a periodic parameterisation $\kappa : [0, 1] \rightarrow \Gamma$ for Γ , we have the integral equation

$$\int_0^1 \frac{i}{4} H_0^{(1)}(k|x - \kappa(\tau)|) e^{ik(g^i(\kappa(\tau)) - g^i(x))} |\nabla \kappa(\tau)| q_s(\tau) d\tau = u_s^i(x). \quad (37)$$

The unknown in (37) is $q_s(\tau)$, defined in the parameter domain for simplicity. The unknown is non-oscillatory, and one can therefore solve (37) using a coarse discretisation for $q_s(\tau)$.

4.3 Asymptotic behaviour of the solution

In the past decades, a lot of effort has been invested in studying the asymptotic behaviour of the solution q to (34) as a function of the wavenumber, concentrating mainly on the scattering of a plane wave (see, e.g., [23, 27] and references therein). For smooth and convex obstacles, there are three important regions with different properties, illustrated in Figure 1: the illuminated region, the shadow region, and the transitional shadow boundary region. In the illuminated region, the scattered wave is described asymptotically by geometrical optics: a wave is reflected such that the angle of incidence and the angle of reflection are identical. A wave tangential to the shadow boundary causes diffraction. The density function decays rapidly away from the shadow boundary into the shadow region, due to the continuous emission of diffracted waves. In the deep shadow region, the density function vanishes.

The asymptotic behaviour of q_s reflects these three regions. Assume an incoming plane wave in the direction α of the form $u^i(x) = e^{ik\alpha \cdot x}$ with $|\alpha| = 1$. It was proved in [27] that q_s has an asymptotic expansion, for $\tau \in [0, 1]$, of the form

$$q_s(\tau) \sim \sum_{m,n \geq 0} k^{2/3-n-2m/3} b_{m,n}(\alpha, \tau) \Psi^{(n)}(k^{1/3} Z(\alpha, \tau)). \quad (38)$$

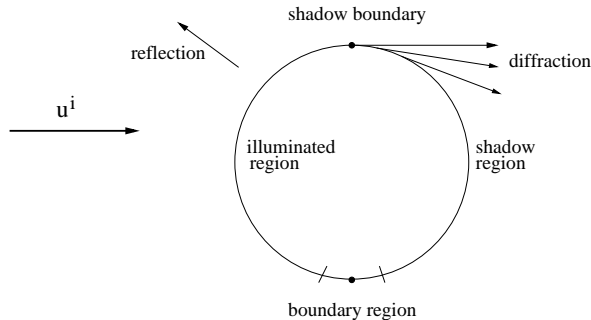


Figure 1: Reflection and diffraction effects in the scattering of an incoming wave u^i by a smooth and convex obstacle.

We recall the main characteristics of this expansion that are needed in our analysis. For a more complete discussion, we refer to [27]. The function $Z \in C^\infty$ is infinitely smooth, and has a simple root at the two shadow boundary points. The shadow boundary points are characterised by $\alpha \cdot \nu = 0$, with ν the exterior normal to Ω . The function Z is positive when $\alpha \cdot \nu < 0$, i.e., in the illuminated region, and negative in the shadow region. The function $\Psi(z)$ is smooth for positive arguments, with

$$\Psi(z) \sim z, \quad z \rightarrow \infty, \quad (39)$$

and exponentially but oscillatory decaying for large negative arguments. This means that, as $k \rightarrow \infty$, we can derive the asymptotic properties from the leading order of (38),

$$|q_s(\tau)| = \begin{cases} O(k), & \text{illuminated region,} \\ O(k^{2/3}), & \text{shadow boundary,} \\ O(e^{-k^{1/3}d(\tau)}), & \text{shadow region.} \end{cases} \quad (40)$$

There is a k -dependent transition region near the shadow-boundary, since the order of the size of q_s changes smoothly from 1 to $2/3$. The behaviour in the shadow region is also k -dependent, as the solution is oscillatory decaying. Motivated by (38), we introduce a transition region of size $O(k^{-1/3})$ around the shadow boundary points, and define the shadow boundary regions as

$$T_{B1}(k) = [t_{sb1} - D_1 k^{-1/3}, t_{sb1} + C_1 k^{-1/3}], \quad (41)$$

$$T_{B2}(k) = [t_{sb2} - C_2 k^{-1/3}, t_{sb2} + D_2 k^{-1/3}], \quad (42)$$

with constants $C_1, C_2, D_1, D_2 > 0$ independent of k , but small enough such that $T_{B1}(k)$ and $T_{B2}(k)$ are non overlapping, and with t_{sb1} and t_{sb2} the locations of the two shadow boundary points in the parameter domain $[0, 1]$. The illuminated region is defined as

$$T_I(k) = (t_{sb1} + C_1 k^{-1/3}, t_{sb2} - C_2 k^{-1/3}). \quad (43)$$

The shadow region is the remaining part of the interval $[0, 1]$.

The size of the transition region is related to the behaviour of the argument $k^{1/3}Z(\omega, \tau)$ of the function $\Psi^{(n)}$ in (38). Since $Z(\omega, \tau)$ has a simple zero at t_{sb1} , we have

$$Z(\omega, \tau) \approx Z'(\omega, t_{sb1})(\tau - t_{sb1}), \quad \tau \rightarrow t_{sb1}.$$

Hence, $|k^{1/3}Z(\omega, \tau)| = O(1)$ for $\tau \in T_{B1}(k)$. We can therefore state

$$|q_s(\tau)| = \begin{cases} O(k), & \tau \in T_I(k), \\ O(k^{2/3}), & \tau \in T_{B1}(k) \cup T_{B2}(k), \\ O(e^{-k^{1/3}d(\tau)}), & \tau \in [0, 1] \setminus (T_I(k) \cup T_{B1}(k) \cup T_{B2}(k)). \end{cases} \quad (44)$$

We also state the size of the first order derivative for further reference,

$$|q'_s(\tau)| = \begin{cases} O(k), & \tau \in T_I(k), \\ O(k), & \tau \in T_{B1}(k) \cup T_{B2}(k). \end{cases} \quad (45)$$

5 A hybrid high frequency boundary element method

The collocation of integral equation (37) in a point x_n leads to a one-dimensional and oscillatory integral in the integration variable τ . In this section, we show how an efficient quadrature rule can be used for the discretisation of that collocation integral. First, we discuss both the classical boundary element approach and a discretisation based on the quadrature rule in §5.1. We show that the quadrature rule can not always be applied in §5.2, and we arrive at a method combining both approaches in §5.3.

5.1 Collocation approach for the discretisation

Consider a collocation scheme for integral equation (37), with a set of N distinct collocation points $x_n = \kappa(t_n)$, $t_n \in [0, 1]$, $n = 1, \dots, N$. The classical way to proceed is to look for an approximation q_c to solution q_s in the form

$$q_c(\tau) = \sum_{m=1}^N c_m \phi_m(\tau), \quad (46)$$

where the ϕ_m functions are a set of linearly independent basis functions. The number of basis functions may be small, since the exact solution q_s is not oscillatory. Collocating equation (37), with q_s replaced by q_c , in the points t_n leads to the equations

$$\int_0^1 \frac{i}{4} H_0^{(1)}(k|\kappa(t_n) - \kappa(\tau)|) e^{ik(g^i(\kappa(\tau)) - g^i(\kappa(t_n)))} |\nabla \kappa(\tau)| q_c(\tau) d\tau = u_s^i(x_n), \quad n = 1, \dots, N. \quad (47)$$

The collocation approach therefore leads to a linear system $Ac = b$ of size $N \times N$, where the elements of the discretisation matrix A are given by

$$A_{n,m} = \int_{\text{supp}(\phi_m)} \frac{i}{4} H_0^{(1)}(k|\kappa(t_n) - \kappa(\tau)|) e^{ik(g^i(\kappa(\tau)) - g^i(\kappa(t_n)))} |\nabla \kappa(\tau)| \phi_m(\tau) d\tau, \quad (48)$$

and the right hand side by $b_n = u_s^i(x_n)$. The discretisation matrix A is dense, but small compared to the classical boundary element discretisation for the original equation. Hence, this is a big improvement over the direct discretisation of (34). Since the elements $A_{n,m}$ are given by oscillatory integrals in (48), they can be computed efficiently using the numerical steepest descent technique described in §2.2. This yields an efficient total solution method, that remains efficient when k increases.

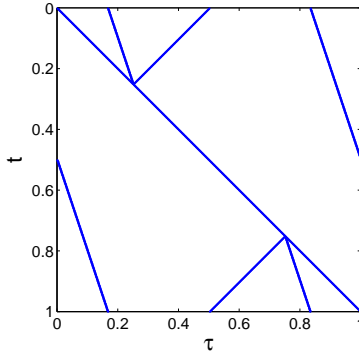


Figure 2: The location of the contributing points of the collocation integral for the scattering of a plane wave by a circular obstacle. Each row corresponds to a fixed value $t \in [0, 1]$, with the shadow boundary points at 0.25 and 0.75, and the illuminated region in between. The singular points are located along the diagonal. The remaining points correspond to stationary points.

However, there are still some issues associated with this approach. Since the matrix is dense, the method requires the evaluation of N^2 integrals. Although N may be rather small, the computational cost can still be high. Interestingly, it was observed in [13] that many of the elements are small, and can in fact be discarded, reducing the computation time. A second, and more important issue is that the results of [13] indicate that the error of the scheme increases with increasing wavenumber. Here, we examine a different discretisation of (47) that aims to address these issues, based on the quadrature rule developed in §3 and motivated by the accuracy of the rules for high wavenumbers. Owing to the small number of required quadrature points, the resulting discretisation matrix will be highly sparse.

Based on the collocation integral (47), we define the oscillatory integral

$$I_c[f; t_n] := \int_0^1 \frac{i}{4} H_0^{(1)}(k|\kappa(t_n) - \kappa(\tau)|) e^{ik(g^i(\kappa(\tau)) - g^i(\kappa(t_n)))} |\nabla \kappa(\tau)| f(\tau) d\tau. \quad (49)$$

The integral $I_c[f; t_n]$ is highly similar to the model integral $I_H[f]$ that was introduced in §3. In particular, one can find a quadrature rule such that

$$I_c[f; t_n] \approx Q_c[f; t_n] := \sum_{i=0}^{l_n} \sum_{j=0}^{d_{n,i}} w_{n,i,j}^c f^{(j)}(\tau_{n,i}). \quad (50)$$

The weights are found by evaluating line integrals $S^c[f; t_n]$ in the complex plane similar to $S^H[f]$. A difference of $Q_c[f; t_n]$ compared to $Q_H[f]$ is the additional factor $\frac{i}{4} |\nabla \kappa(\tau)|$ in the integrand. Assuming an analytic parameterisation κ , this factor can simply be included in the weight function of the rule. Hence, the construction and the convergence properties of $Q_c[f; t_n]$ are described by the corresponding analysis for $Q_H[f]$ in §3. The weights $w_{n,i,j}^c$ depend on k and on t_n , the constants l_n and $d_{n,i}$ and the points $\tau_{n,i}$ depend on t_n only.

The quadrature points are found from the oscillator. The oscillator of (49) is known explicitly; it is given by

$$g(\tau; t_n) = \sqrt{(\kappa_1(t_n) - \kappa_1(\tau))^2 + (\kappa_2(t_n) - \kappa_2(\tau))^2} + g^i(\kappa_1(\tau), \kappa_2(\tau)) - g^i(\kappa_1(t_n), \kappa_2(t_n)), \quad (51)$$

with $\kappa(t) = (\kappa_1(t), \kappa_2(t))$. The quadrature points $\tau_{n,i}$ of $Q_c[f; t_n]$ are the points τ where the integrand becomes singular (and hence non-analytic), and the stationary points of the oscillator $g(\tau; t_n)$. These points are derived by a straightforward, but technical analysis of $g(\tau; t_n)$. There are no contributing endpoints, as the integrand is periodic on the closed curve Γ . The location of the quadrature points is illustrated in Figure 2 for the scattering of a plane wave by a circular obstacle. There is one stationary point if t_n lies in the illuminated region, and there are three stationary points if t_n lies in the shadow region. Two of these points coalesce into one stationary point of order $r = 2$ exactly at the shadow boundary. Figure 2 is illustrative for more general convex shapes and incoming waves. If the incoming wave is not a plane wave however, then the point where two stationary points coalesce may differ from the point where the incoming wave is tangential to the boundary. In the following, we consistently use the term *shadow boundary* to refer to the point where two stationary points coalesce into one, as that point determines the numerical properties of the scheme.

We now describe how the quadrature rule (50) can be used in the discretisation. The derivatives of q_c can be written in terms of the basis functions ϕ_m ,

$$q_c^{(j)}(\tau) = \sum_{m=1}^N c_m \phi_m^{(j)}(\tau).$$

Hence, applying the quadrature rule to q_c yields a matrix B with entries

$$B_{n,m} = \begin{cases} \sum_{i: \tau_{n,i} \in \text{supp}(\phi_m)} \sum_{j=0}^{d_{n,i}} w_{n,i,j}^c \phi_m^{(j)}(\tau_{n,i}), & \exists i \in [0, l_n] : \tau_{n,i} \in \text{supp}(\phi_m), \\ 0 & \text{otherwise} \end{cases} \quad (52)$$

The entry $B_{n,m}$ is nonzero only if at least one quadrature point $\tau_{n,i}$ exists that lies in the support of the basis function ϕ_m . The number of nonzero points therefore depends on the size of the supports of the basis functions. If all basis functions are local, then the structure of B will resemble the structure shown in Figure 2.

However, the value $Q_c[q_c; t_n]$ is not always a good approximation for the collocation integral (47). It turns out that the quadrature rule can not always be used, depending on the collocation point t_n . Therefore, we first examine the accuracy of $Q_c[q_c; t_n]$. We will formulate a combined approach in §5.3 that uses the quadrature rule only where it is sufficiently accurate.

5.2 Convergence of the specialised quadrature rule as a function of k

The convergence of quadrature rule $Q_c[f; t_n]$ as a function of k can be derived from the results for $Q_H[f]$ discussed in §3.3. These results were derived with the assumption that the function f is independent of k . The solution q_s of integral equation (37) depends on k ; an important issue in the derivation of our hybrid scheme is what can be said about the accuracy of the quadrature rule $Q_c[q_s; t_n]$ when applied to the exact solution q_s . As it turns out, in that case, the accuracy of the rule depends on the location of the quadrature points.

First, we consider the case of a function that is independent of k . We will show that for a given collocation point t_n and a given value of i , the quadrature point $\tau_{n,i}$ yields a contribution to the value of Q_c in (50) with an accuracy that increases with k . Define the partial sums

$$S(d; f, n, i) = \sum_{j=0}^d w_{n,i,j}^c f^{(j)}(\tau_{n,i}).$$

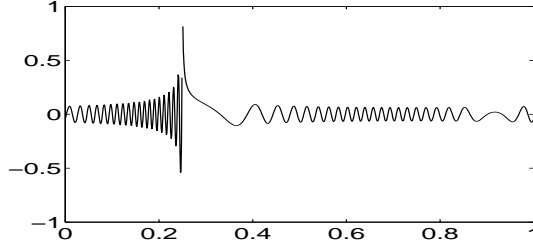


Figure 3: The real part of the integrand for $t_n = t_{sb1}$ for a circular obstacle and $k = 100$.

The definition of S is such that one can write $Q_c[f; t_n] = \sum_{i=0}^{l_n} S(d_{n,i}; f, n, i)$, where $l_n + 1$ is the total number of quadrature points for a given collocation point t_n . The partial sum $S(d_{n,i}; f, n, i)$ may be regarded as the contribution of the quadrature point $\tau_{n,i}$ to the total value of the quadrature approximation. This local contribution converges to a fixed value $s(k)$ for increasing d , and the convergence becomes faster with increasing k . In order to see this, consider a point $\tau_{n,i}$ that is not a stationary point. By Lemma 3.3, we have $w_{n,i,j}^c = O(k^{-j-3/2})$. If f is independent of k , it follows that

$$|S(d+1; f, n, i) - S(d; f, n, i)| = O(k^{-(d+1)-3/2}). \quad (53)$$

The error of the partial sum using d derivatives decreases with increasing k .

When the function f depends on k , the asymptotic behaviour of f and its derivatives at $\tau_{n,i}$ should be included in the derivation of estimate (53). We shall elaborate this for the case of f equal to the exact solution q_s . The necessary information for this elaboration was derived in §4.3. We will show that the error of the quadrature rule may actually be $O(1)$ in k , depending on the location of the quadrature points $\tau_{n,i}$.

Consider first the case $\tau_{n,i} \in T_I(k)$, i.e., the quadrature point lies in the illuminated region. If $\tau_{n,i} = t_n$, then $\tau_{n,i}$ is a singular point. From Lemma 3.3, we have $|w_{n,i,0}^c| = O(k^{-1})$ and $|w_{n,i,1}^c| = O(k^{-2})$. We have $|q_s(\tau_{n,i})| = O(k)$ from (44) and $|q'_s(\tau_{n,i})| = O(k)$ from (45). Combined, this yields the estimate

$$|S(1; q_s, n, i) - S(0; q_s, n, i)| = O(k^{-1}), \quad \tau_{n,i} = t_n \in T_I(k).$$

This means that the accuracy increases with increasing k : the error when using only the first term scales as $O(k^{-1})$. Using Lemma 3.4, it can be found that the error of the first term for a stationary point $\tau_{n,i} \neq t_n$ is $O(k^{-1/2})$.

Next, consider the case $\tau_{n,i} \in T_{B1}(k)$. At the shadow boundary $\tau_{n,i} = t_n = t_{sb1}$, we have $|w_{n,i,0}^c| = O(k^{-2/3})$ and $|w_{n,i,1}^c| = O(k^{-1})$ from Lemma 3.4, and $|q_s(t_n)| = O(k^{2/3})$ and $|q'_s(t_n)| = O(k)$ from (44) and (45). The exponents cancel exactly; we have

$$|S(1; q_s, n, i) - S(0; q_s, n, i)| = O(1), \quad \tau_{n,i} = t_{sb1}.$$

The accuracy of the contribution $S(d; f, n, i)$ does not improve with increasing k for a fixed d , although the partial sum may still converge if more derivatives are used. Similar observations hold for $\tau_{n,i} \neq t_{sb1}$ in the shadow boundary region. It turns out that the quadrature rule is not as useful in the shadow boundary region as in the illuminated region.

There is however an important remark that can be made here. Due to the square root in the definition (51) of the oscillator, the singular point $\tau_{n,i} = t_n$ is a branch point of the oscillator.

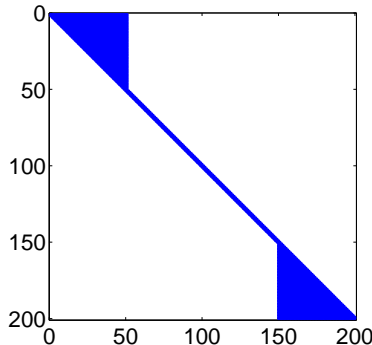


Figure 4: Illustration of the sparse discretisation matrix using cubic B-splines for the scattering of a plane wave by a circular obstacle. The middle part of the matrix is tridiagonal.

A consequence is that the left and right limit of the derivatives of the oscillator may differ. Indeed, the oscillator has a stationary point of order $r = 2$ at $t_n = t_{sb1}$ only in the right limit. The left limit of the derivative of the oscillator is nonzero. This is illustrated in Figure 3: the integrand is highly oscillatory to the left of the shadow boundary, and not oscillatory to the right. It turns out that the quadrature rule can be used on the left interval $[0, t_{sb1}]$ and in the illuminated region. It is not suited for the intermediate interval $[t_{sb1}, t_{sb1} + C_1 k^{-1/3}]$. Due to the stationary point, the integrand is not oscillatory in that interval.

5.3 A sparse discretisation

The basis functions for the discretisation are chosen corresponding to the behaviour of the solution in the three different regions identified in §4.3. Recall that the solution is smooth in the illuminated region, and oscillatory but exponentially decaying in the shadow region. First, following [7], we approximate the solution by zero in the shadow region. We choose a fixed number of basis functions in the illuminated region. Finally, we also choose a fixed number of basis functions in the transitional shadow boundary region, independently of k . Based on the asymptotic expansion (38), one can see that this corresponds to using a fixed number of basis functions per oscillation of the solution. It was already noted in §4.3 that the argument $k^{1/3}Z(\alpha, \tau)$ of the function Ψ is bounded in k , $\tau \in T_{B1}(k)$. The oscillatory behaviour of the exact solution q_s in $T_{B1}(k)$ is due to the oscillations of Ψ for negative arguments. Since the argument of Ψ is bounded, the number of possible oscillations is also bounded, independently of k .

In our implementation, we have chosen to use cubic B-splines as basis functions. The nodes of the splines are the collocation points of the collocation method. They are chosen equidistantly in the regions $T_{B1}(k)$, $T_{B2}(k)$ and $T_I(k)$. Owing to the small number of quadrature points $\tau_{n,i}$ for each collocation point t_n , the discretisation matrix is highly sparse. Since the quadrature rule, applied to the exact solution q_s , may not provide sufficient accuracy for quadrature points in the shadow boundary region, we propose the following scheme.

If $t_n \in T_I(k)$, then

- the quadrature rule is applied for the singular point in the illuminated region,

- the stationary points lie in the shadow region, and they are discarded.

For cubic splines, the singular point t_n lies in the support of only three separate basis functions. The three corresponding matrix entries are given by (52). The contributions of the stationary points are discarded because the solution is approximated by zero in the shadow region.

If $t_n \in T_{B_1}(k)$, then

- the quadrature rule is applied on the interval $[0, t_n]$,
- a classical dense discretisation is used on the interval $[t_n, t_{sb1} + C_1 k^{-1/3}]$,
- the quadrature rule is applied on the interval $[t_{sb1} + C_1 k^{-1/3}, 1]$.

The quadrature rule on $[0, t_n]$ reduces to the contribution of the singular point t_n . The corresponding weights have the form of (25) with S_l^H replaced by S_i^c ,

$$w_{n,s,j}^c = -S_{i_s}^c \left[\frac{(x - t_n)^j}{j!}; t_n \right],$$

where i_s is the index such that $t_n = \tau_{n,i_s}$. The quadrature rule on $[t_{sb1} + C_1 k^{-1/3}, 1]$ consists of the contributions of the stationary points $\tau_{n,i}$ outside the shadow boundary region, and of the endpoint $t_r := t_{sb1} + C_1 k^{-1/3}$. The weights corresponding to that endpoint have the form of (23),

$$w_{n,r,j}^c = S_{i_r+1}^c \left[\frac{(x - t_r)^j}{j!}; t_r \right],$$

where i_r is the index such that $t_r \in [\tau_{n,i_r}, \tau_{n,i_r+1}]$. Finally, the dense discretization in the interval $[t_n, t_r]$ leads to elements of the form

$$\sigma_{n,m} = \int_{\text{supp}(\phi_m) \cap [t_n, t_r]} \frac{i}{4} H_0^{(1)}(k|\kappa(t_n) - \kappa(\tau)|) e^{ik(g^i(\kappa(\tau)) - g^i(\kappa(t_n)))} |\nabla \kappa(\tau)| \phi_m(\tau) d\tau, \quad (54)$$

The only difference compared to (48) is that the integration domain may be cut at the boundaries of $[t_n, t_r]$. Summarizing, the elements of the discretisation matrix for $t_n \in T_{B_1}(k)$ can be written as

$$C_{n,m} = \begin{cases} \sigma_{n,m} & \text{if } \text{supp}(\phi_m) \cap [t_n, t_r] \neq \emptyset \\ + \sum_{j=0}^{d_{n,i_s}} w_{n,s,j}^c \phi_m^{(j)}(t_n) & \text{if } t_n \in \text{supp}(\phi_m) \\ + \sum_{j=0}^{d_{n,i_r}} w_{n,r,j}^c \phi_m^{(j)}(t_r) & \text{if } t_r \in \text{supp}(\phi_m) \\ + \sum_{i: t_r < \tau_{n,i} \in \text{supp}(\phi_m)} \sum_{j=0}^{d_{n,i}} w_{n,i,j}^c \phi_m^{(j)}(\tau_{n,i}), & \exists i \in [0, l_n] : t_r < \tau_{n,i} \in \text{supp}(\phi_m), \\ \sum_{i: t_r < \tau_{n,i} \in \text{supp}(\phi_m)} \sum_{j=0}^{d_{n,i}} w_{n,i,j}^c \phi_m^{(j)}(\tau_{n,i}), & \exists i \in [0, l_n] : t_r < \tau_{n,i} \in \text{supp}(\phi_m), \\ 0 & \text{otherwise.} \end{cases}$$

The case $t_n \in T_{B_2}(k)$ can be treated similarly. The structure of the sparse matrix C is illustrated in Figure 4. The two small dense parts correspond to the dense discretisation in the intervals $[t_n, t_{sb1} + C_1 k^{-1/3}]$ and $[t_{sb2} - C_2 k^{-1/3}, t_{sb2}]$. For simplicity, we have chosen the constant C_1 large enough such that, for $t_n \in T_{B_1}$, all stationary points $\tau_{n,i} \in T_{B_1}(k)$ also lie in the shadow boundary region. The constant C_2 was chosen similarly. One can show that the

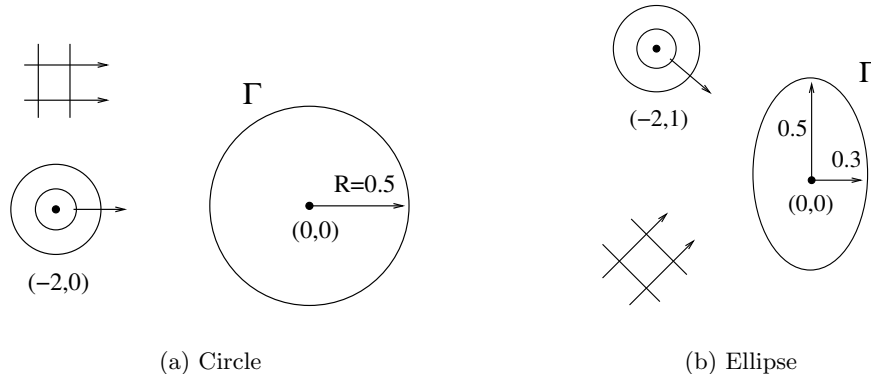


Figure 5: Illustration of two smooth convex scattering obstacles. The boundary conditions are plane waves, or circular waves originating from a point source.

required integrals of the form (54) are not oscillatory. Due to the stationary point of order $r = 2$, the integrand behaves as $e^{ikc(\tau - t_{sb1})^3}$. The argument of the exponential is bounded in k , since by construction we have

$$|\tau - t_{sb1}| \leq \max\{C_1, D_1\}k^{-1/3}.$$

Hence, there is only a bounded number of oscillations in the integrals for increasing k . The integrals can therefore be evaluated with a number of operations that is independent of k . Since the weights of the quadrature rule can be evaluated efficiently as well, and because the number of unknowns is fixed, the matrix in Figure 4 can be computed with a total number of operations that is independent of k .

6 Numerical results

6.1 Convergence and total solution time

We consider the scattering by two convex obstacles, a circle and an ellipse, shown in Figure 5. We use two types of boundary conditions: a plane wave, modelled in the form $u^i(x) = e^{ik\alpha \cdot x}$, and a point source, modelled by $u^i(x) = H_0^{(1)}(|x - x_0|)$, with x_0 a point in the exterior Ω^+ of the obstacle. The circle and ellipse are parameterised by

$$\kappa(t) = \begin{cases} R \cos(2\pi t) \\ R \sin(2\pi t) \end{cases} \quad \text{and} \quad \kappa(t) = \begin{cases} R_1 \cos(2\pi t) \\ R_2 \sin(2\pi t) \end{cases}$$

respectively. The boundary conditions for the ellipse are deliberately chosen to yield a non-symmetric problem. We use N cubic B-spline basis functions, defined on the interval $[t_{sb1} - D_1k^{-1/3}, t_{sb2} + D_2k^{-1/3}]$. A fixed number N_1 of these functions are defined on the shadow boundary regions T_{B1} and T_{B2} . The collocation points are the nodes of the spline function, chosen equidistantly in the intervals T_{B1} , T_I and T_{B2} respectively.

The smooth function q_c is illustrated in Figure 6 for the different scattering problems. The mild oscillatory behaviour of the function near the shadow boundary is illustrated in the left panel of Figure 7, showing only the real part of the solution. Two spikes are present near the

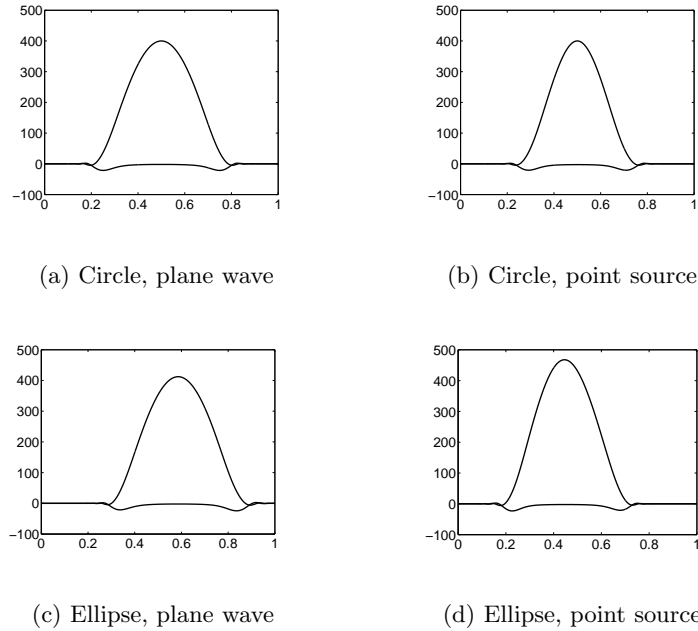


Figure 6: The real and imaginary part of the smooth function q_s for different scattering problems. The real part is the lower curve in each example. The wavenumber is $k = 200$.

shadow boundary, with a peak value that scales as $O(k^{2/3})$ as predicted by our estimate (40). The dashed line shows the effect of doubling k . The $O(k)$ behaviour in the illuminated region is clear from the imaginary part illustrated in the right panel of Figure 7

Table 2 shows the timings for an implementation of the algorithm of §5.3 in Matlab. In all examples considered, the time actually decreases with increasing wavenumber k . This is due to the fact that, at larger frequencies, the weights of the specialised quadrature rule $Q_c[f; t_n]$ are easier to compute. In a classical boundary element method, and using 10 unknowns per wavelength, the case $k = 100000$ corresponds to a dense matrix with $N = 500000$ unknowns.

Table 2: Total solution time in seconds for the different scattering problems. All parameters are kept fixed, except the wavenumber k . We used $d = 2$ derivatives and $N = 150$ unknowns.

k	Circle		Ellipse	
	Plane wave	Point source	Plane wave	Point source
200	232s	546s	322s	616s
400	226s	531s	308s	596s
800	224s	525s	303s	589s
1600	221s	521s	299s	583s
10000	217s	505s	290s	567s
100000	211s	495s	272s	542s

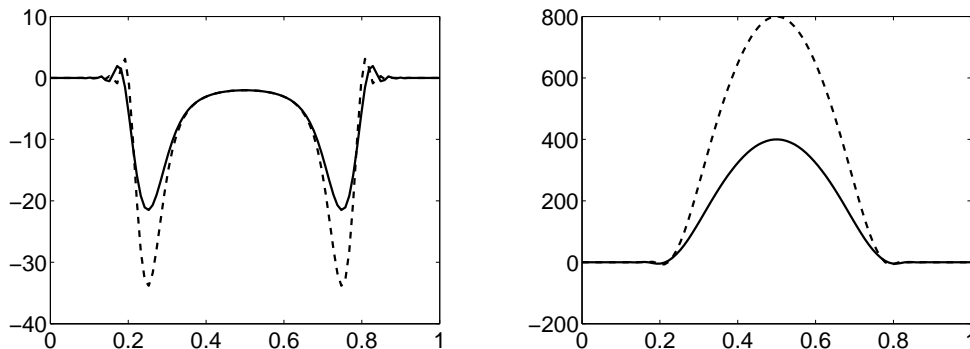
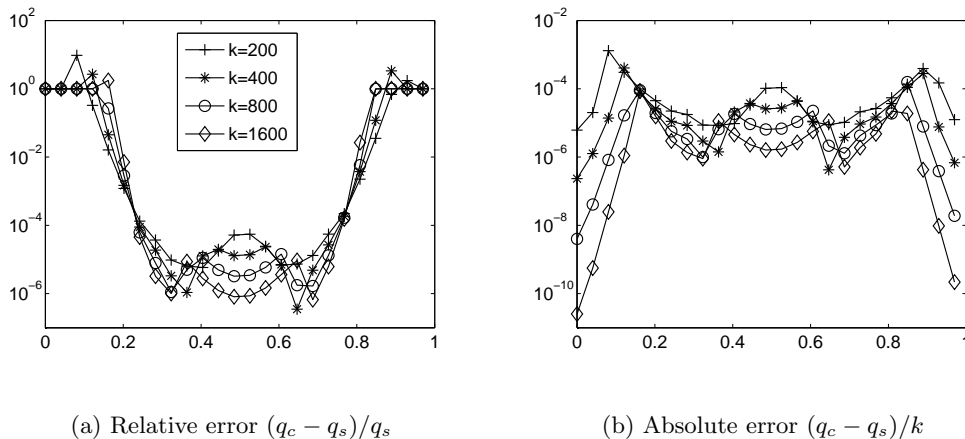


Figure 7: The real part (left) and imaginary part (right) of q_s for the scattering of a plane wave by a circle. The dense line corresponds to $k = 200$, the dashed line to $k = 400$.



(a) Relative error $(q_c - q_s)/q_s$

(b) Absolute error $(q_c - q_s)/k$

Figure 8: Absolute and relative error for the scattering of a plane wave by a circle for different values of k . We have used $d = 1$ derivative in the quadrature rule $Q_c[f; t]$.

6.2 Error of the solution

In applications, one is usually interested in the quantity q_s/k . For example in electromagnetics, the quantity q_s/k is proportional to the induced current on the surface of the obstacle, with a proportionality constant that is independent of k . The exact solution q_s of the scattering problem is known only for the case of scattering of a plane wave by a circle. The relative error $(q_c - q_s)/q_s$ and the absolute error $(q_c - q_s)/k$ for this case are illustrated in Figure 8 for a number of different values for k . We have chosen to use derivatives up to order $d_{n,i} = d = 1$ in each quadrature rule for this example. The error decreases rapidly with increasing k in the illuminated region. This is due to the higher accuracy of the quadrature rule $Q_c[f; t]$ at larger frequencies. The relative error tends to 100% in the deep shadow region because we have approximated the solution by 0 in that region. One can verify from the figures that the absolute error in that region is still quite small compared to the average value of the function $q_s(\tau)$.

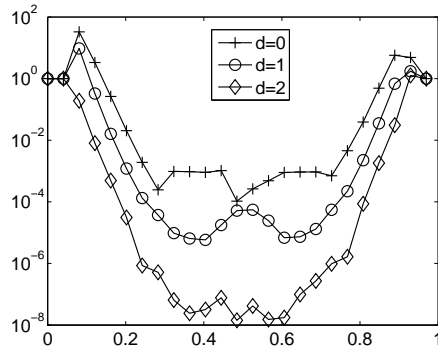


Figure 9: Comparison of the relative error for different values of d , the number of derivatives used in the quadrature rule $Q_c[f; t]$.

It is important to know how the error can be controlled, i.e., how the parameters of the method can be chosen to achieve a given accuracy. The parameters are:

- N, N_1 : the total number of unknowns, and the number of unknowns in the shadow boundary region respectively;
- C_1, C_2, D_1, D_2 : these parameters control the size of the shadow boundary region in definitions (41)-(43);
- $d_{n,i}$: the number of derivatives used in the quadrature rule $Q_c[f; t_n]$ given by (50).

Increasing each of these parameters decreases the error, although the effect of increasing each parameter independently is bounded. For example, increasing N indefinitely does not yield arbitrary accuracy, because the accuracy of the quadrature rule is independent of N . The constants C_1, C_2, D_1 and D_2 can be chosen so large that the shadow boundary region covers the whole boundary. In that case, the method almost reduces to the regular boundary element method. The accuracy of the quadrature rule is increased by increasing $d_{n,i}$. We have considered a fixed number of derivatives $d = d_{n,i}$ in each example. Figure 9 shows the relative error for different values of d . The accuracy of the method greatly increases with increasing d , while the sparsity structure of the matrix remains exactly the same. For a cubic spline, $d = 2$ is the largest possible value since higher order derivatives are discontinuous.

Finally, we note that the matrices are well conditioned. The matrices that were constructed to produce the results in Table 2 have size 150×150 . The largest condition number in these example was 167. Since the matrices are small, the corresponding system of equations can be readily solved using a direct solver.

7 Concluding remarks

The method presented in this paper achieves a sparse discretisation matrix for an integral equation, which is made possible by the presence of strong oscillations. The method is based on a classical boundary element technique near the shadow boundary, and uses a new quadrature formula in the illuminated region. The a priori knowledge of the phase of the solution

allows a discretisation with a fixed, small number of unknowns. The new quadrature rule yields a sparse discretisation matrix. Moreover, the accuracy of the solution in the illuminated region increases with increasing frequency.

The method can still be improved in a number of ways. For example, we have only considered the localised Filon-type method, while numerical experiments indicate that regular Filon-type methods are typically more accurate for the same frequency. One could also add additional quadrature points besides the singular and stationary points to improve the accuracy. The small, densely discretised part near the shadow boundary may possibly be avoided by using a more elaborate ansatz for the asymptotic behaviour of the solution, such as those described by the Geometric Theory of Diffraction [17, 23, 13].

The method is limited to smooth convex obstacles. The approach of [7] for smooth convex obstacles can be extended to multiple scattering configurations using an iterative approach [12]. We expect the same will hold for our approach. The extension to three-dimensional problems is the subject of future research. This will be based on suitable cubature rules for multivariate highly oscillatory integrals which have recently been constructed [18].

References

- [1] T. Abboud, J. Nédélec, and B. Zhou. Méthode des équations intégrales pour les hautes fréquences. *C. R. Acad. Sci. Paris*, 318:165–170, 1994.
- [2] K. R. Aberegg and A. F. Peterson. Application of the Integral Equation-Asymptotic Phase method to two-dimensional scattering. *IEEE Trans. Antennas Propagat.*, 43(5):534–537, 1995.
- [3] M. Abramowitz and I. A. Stegun. *Handbook of mathematical functions with formulas, graphs, and mathematical tables*. Dover Publications, New York, 1965.
- [4] P. Bettess. Short wave scattering, problems and techniques. *Phil. Trans. R. Soc. Lond. A*, 362:421–443, 2004.
- [5] N. Bleistein. Asymptotic expansions of integral transforms of functions with logarithmic singularities. *SIAM J. Math. Anal.*, 8(4):655–672, 1977.
- [6] N. Bleistein and R. Handelsman. *Asymptotic Expansions of Integrals*. Holt, Rinehart and Winston, 1975.
- [7] O. Bruno, C. Geuzaine, J. Monro, and F. Reitich. Prescribed error tolerances within fixed computational times for scattering problems of arbitrarily high frequency: the convex case. *Phil. Trans. R. Soc. Lond. A*, 362(1816):629–645, 2004.
- [8] D. Colton and R. Kress. *Integral Equation Methods in Scattering Theory*. Wiley, New York, 1983.
- [9] E. Darve. The fast multipole method: Numerical implementation. *J. Comput. Phys.*, 160(1):195–240, 2000.
- [10] P. J. Davis and P. Rabinowitz. *Methods of Numerical Integration*. Computer Science and Applied Mathematics. Academic Press Inc., 1984.

- [11] V. Domínguez, I. G. Graham, and V. P. Smyshlyaev. A hybrid numerical-asymptotic boundary integral method for high-frequency acoustic scattering. Technical Report BICSP 1/06, University of Bath, 2006.
- [12] C. Geuzaine, O. Bruno, and F. Reitich. On the $O(1)$ solution of multiple-scattering problems. *IEEE Trans. Magn.*, 41(5):1488–1491, 2005.
- [13] E. Giladi. Asymptotically derived boundary element method for the Helmholtz equation. In *Proceedings of the 7th International Conference on Mathematical and Numerical Aspects of Wave Propagation (WAVES2005)*, pages 420–422, 2005.
- [14] E. Giladi and J. B. Keller. A hybrid numerical asymptotic method for scattering problems. *J. Comput. Phys.*, 174(1):226 – 247, 2001.
- [15] L. Greengard and V. Rokhlin. A fast algorithm for particle simulations. *J. Comput. Phys.*, 73(2):325–348, 1987.
- [16] R. Harrington and J. Mautz. H-field, E-field and combined field solution for conducting bodies of revolution. *Arch. Elektron. Übertragungstechn.*, 32(4):157–164, 1978.
- [17] R. F. Harrington. *Time-harmonic electromagnetic fields*. McGraw-Hill, 1961.
- [18] D. Huybrechs and S. Vandewalle. The construction of cubature rules for multivariate highly oscillatory integrals. Technical Report TW442, K.U. Leuven, 2005.
- [19] D. Huybrechs and S. Vandewalle. On the evaluation of highly oscillatory integrals by analytic continuation. *SIAM J. Numer. Anal.*, 2006. To appear.
- [20] A. Iserles and S. Nørsett. On quadrature methods for highly oscillatory integrals and their implementation. *BIT*, 44(4):755–772, 2004.
- [21] A. Iserles and S. Nørsett. Efficient quadrature of highly oscillatory integrals using derivatives. *Proc. Royal Soc. A*, 461:1383–1399, 2005.
- [22] A. Iserles, S. P. Nørsett, and S. Olver. Highly oscillatory quadrature: the story so far. Technical Report NA2005-06, University of Cambridge, 2005.
- [23] J. Keller. Geometrical theory of diffraction. *J. Opt. Soc. Am.*, 52:116–130, 1962.
- [24] S. Langdon and S. N. Chandler-Wilde. Implementation of a boundary element method for high frequency scattering by convex polygons. In K. Chen, editor, *Proc. 5th U.K. Conf. on Boundary Integral Methods*, pages 2–11, 2005.
- [25] S. Langdon and S. N. Chandler-Wilde. A wavenumber independent boundary element method for an acoustic scattering problem. *SIAM J. Numer. Anal.*, 43(6):2450–2477, 2006.
- [26] D. Levin. Fast integration of rapidly oscillatory functions. *J. Comput. Appl. Math.*, 67(1):95–101, 1996.
- [27] R. B. Melrose and M. E. Taylor. Near peak scattering and the corrected Kirchhoff approximation for a convex obstacle. *Adv. in Math.*, 55(3):242–315, 1985.

- [28] J.-C. Nédélec. *Acoustic and Electromagnetic Equations*, volume 144 of *Applied Mathematical Sciences*. Springer, 2001.
- [29] S. Olver. Moment-free numerical integration of highly oscillatory functions. *IMA J. Num. Anal.*, 2005. To appear.
- [30] E. Stein. *Harmonic analysis: Real-variable methods, orthogonality and oscillatory integrals*. Princeton University Press, Princeton, New York, 1993.
- [31] G. N. Watson. Harmonic functions associated with the parabolic cylinder. *Proc. London Math. Soc. Series 2*, 17:116–148, 1918.